

Néel Temperature of Quasi-Low-Dimensional Heisenberg Antiferromagnets

C. Yasuda¹, S. Todo², K. Hukushima³, F. Alet^{4,5,6}, M. Keller⁴, M. Troyer^{4,5}, and H. Takayama⁷

¹ *Department of Physics, Aoyama Gakuin University, Sagamihara 229-8558, Japan*

² *Department of Applied Physics, University of Tokyo, Tokyo 113-8656, Japan*

³ *Department of Basic Science, University of Tokyo, Tokyo 153-8902, Japan*

⁴ *Theoretische Physik, Eidgenössische Technische Hochschule, CH-8093 Zürich, Switzerland*

⁵ *Computational Laboratory, Eidgenössische Technische Hochschule, CH-8092 Zürich, Switzerland*

⁶ *Service de Physique Théorique, CEA Saclay, 91191 Gif sur Yvette, France and*

⁷ *Institute for Solid State Physics, University of Tokyo, Kashiwa 277-8581, Japan*

(Dated: October 29, 2018)

The Néel temperature, T_N , of quasi-one- and quasi-two-dimensional antiferromagnetic Heisenberg models on a cubic lattice is calculated by Monte Carlo simulations as a function of inter-chain (inter-layer) to intra-chain (intra-layer) coupling J'/J down to $J'/J \simeq 10^{-3}$. We find that T_N obeys a modified random-phase approximation-like relation for small J'/J with an effective universal renormalized coordination number, independent of the size of the spin. Empirical formulae describing T_N for a wide range of J' and useful for the analysis of experimental measurements are presented.

While genuinely one-dimensional (1D) and two-dimensional (2D) antiferromagnetic Heisenberg (AFH) models cannot display long-range order (LRO) except at zero temperature [1], weak inter-chain or inter-layer couplings, J' , which always exist in real materials, lead to a finite Néel temperature T_N . So far, the J' -dependence of T_N was calculated by exactly treating effects of the strong interaction J in the 1D or 2D system, but using mean-field approximations for the inter-chain and inter-layer coupling J' [2]. Recently, more advanced theories of the latter effects have been proposed for quasi-1D (Q1D) [3, 4] and quasi-2D (Q2D) [5] systems, and the results have been compared with the experimental observations on Q1D antiferromagnets, e.g., Sr_2CuO_3 [6], and Q2D antiferromagnets, e.g., La_2CuO_4 [7]. In view of the importance of experimentally well-studied Q2D antiferromagnets as undoped parent compounds of the high-temperature superconductors, accurate and unbiased numerical results for Q1D and Q2D AFH models are strongly desired. In a recent work along this line, Sengupta *et al.* [8] have demonstrated peculiar temperature dependences of the specific heat in the quantum Q2D AFH model.

Here we calculate the Néel temperature T_N as a function of J' in fully three-dimensional (3D) classical and quantum Monte Carlo (MC) simulations of coupled-chains and coupled-layers. Our MC results on the quantum spin- S and classical $S = \infty$ AFH models are analyzed by a modified random-phase approximation (RPA) with a renormalized coordination number defined by

$$\zeta(J') \equiv \frac{1}{J' \chi_s(T_N(J'))}, \quad (1)$$

where $\chi_s(T)$ is the staggered susceptibility of the 1D or 2D model at temperature T .

In a simple RPA calculation [2], this quantity is just the coordination number z_d in the inter-chain or inter-layer directions: $z_1 = 4$ and $z_2 = 2$ for the Q1D and Q2D

systems, respectively. Our main result is that $\zeta(J')$ evaluated by Eq. (1) with our numerically obtained $T_N(J')$ and $\chi_s(T)$ becomes constant

$$\zeta(J') \approx \zeta_d = k_d z_d \quad (2)$$

for $J' < J'_c \simeq 0.1J$, with the constants $k_1 = 0.695$ and $k_2 = 0.65$. These constants k_d differ from the simple RPA result $k_d = 1$, but the value of k_1 is consistent with the modified self-consistent RPA theory for the quantum Q1D (q-Q1D) model of Irkhin and Katanin (IK) [3]. Furthermore we find, that, within our numerical accuracy, the value of k_d is the same for the $S = 1/2$, $S = 1$, $S = 3/2$ and $S = \infty$, and we conjecture that k_d is universal and independent of the spin S for small J'/J .

We also propose empirical formulae for $T_N(J')$ for all values of J' examined in the present work up to $J' = J$ where corrections to the modified RPA are significant quantitatively. These formulae are useful in analyzing experimental results on infinite-layer antiferromagnets such as $\text{Ca}_{0.85}\text{Sr}_{0.15}\text{CuO}_2$ [9], $(5\text{CAP})_2\text{CuBr}_4$ and $(5\text{MAP})_2\text{CuBr}_4$ [10], where they allow to determine the strength of the inter-chain or inter-layer coupling J' from experimental measurements of T_N .

Model and numerical methods.— The Hamiltonian of the Q1D and Q2D AFH models is defined on an anisotropic simple cubic lattice:

$$\mathcal{H} = \sum_{i,j,k} (J_x \mathbf{S}_{i,j,k} \cdot \mathbf{S}_{i+1,j,k} + J_y \mathbf{S}_{i,j,k} \cdot \mathbf{S}_{i,j+1,k} + J_z \mathbf{S}_{i,j,k} \cdot \mathbf{S}_{i,j,k+1}), \quad (3)$$

where the summation $\sum_{i,j,k}$ runs over all the lattice sites on an $L_x \times L_y \times L_z$ cubic lattice and $\mathbf{S}_{i,j,k}$ is the spin operator at site (i, j, k) . We put $J_x = J_y = J'$ and $J_z = J$ for the Q1D model and $J_x = J_y = J$ and $J_z = J'$ for the Q2D model with $J > 0$ and $0 \leq J' \leq J$. For comparison, we also examine the classical limit $S = \infty$ of Eq. (3). Note that $JS(S+1)$ sets the energy scale in the classical

TABLE I: Néel temperatures of the $S = 1/2$ q-Q1D, c-Q1D, $S = 1/2$ q-Q2D, and c-Q2D AFH models, normalized by $JS(S+1)$. The result for the classical system with $J'/J = 1$ is taken from Ref. [14].

J'/J	$T_N/JS(S+1)$			
	q-Q1D	c-Q1D	q-Q2D	c-Q2D
1	1.2589(1)	1.4429(1)	1.2589(1)	1.4429(1)
0.5	0.78997(8)	0.9317(1)	1.0050(4)	1.1733(1)
0.1	0.22555(3)	0.39551(8)	0.6553(4)	0.8526(1)
0.05	0.12171(5)	0.28377(4)	0.5689(2)	0.7797(1)
0.02	0.05258(1)	0.18361(3)	0.48463(8)	0.7115(1)
0.01	0.02768(1)	0.13157(2)	0.43515(6)	0.6731(2)
0.005		0.09393(2)	0.39513(4)	0.6419(2)
0.001		0.042547(6)	0.32571(8)	0.5858(4)

model. In practice, we simulate a system of unit vectors, which is equivalent to fixing $JS(S+1)$ to unity.

The MC simulations have been performed using the continuous-imaginary-time loop algorithm [11] for the quantum model (QMC) and the Wolff cluster algorithm [12] for the classical model (CMC). The AF correlation length ξ_α in each of the directions α ($= x, y, z$) are evaluated by the second-moment method [13] on lattices whose aspect ratio is chosen such that ξ_α/L_α does not depend on α in the vicinity of T_N . Explicitly, for the $S = 1/2$ q-Q1D systems with $J'/J = 0.01, 0.05, 0.1$, and 0.5 , we set $L_z/L_x = 36$ ($L_z \leq 504$), 12 (384), 4 (200), and 2 (128), respectively, while for the $S = 1/2$ quantum Q2D (q-Q2D) systems with $J'/J = 0.001, 0.005, 0.01$, and ≥ 0.02 , we set $L_x/L_z = 48$ ($L_x \leq 288$), 20 (240), 16 (192), and 1 (80), respectively. Then we determine T_N from finite-size scaling, looking for the best data collapse of ξ_α/L_α plotted versus $(T - T_N)L^{1/\nu}$ for different system sizes. We have fixed the exponent $\nu = 0.71$ [14] to the value of the 3D classical Heisenberg universality class. The values of T_N obtained for the $S = 1/2$ q-Q1D and classical Q1D (c-Q1D) systems, and the $S = 1/2$ q-Q2D and classical Q2D (c-Q2D) systems are listed in Table I.

Q1D systems.— The classical 1D (c-1D) model shows LRO at $T = 0$, while the ground state of the $S = 1/2$ and $S = 3/2$ quantum 1D (q-1D) model is gapless and has no LRO [15]. Correspondingly, the staggered susceptibility χ_s for the classical model, given exactly by [16]

$$\chi_s(T) = \frac{x}{3J} \frac{1 + 1/\tanh x - 1/x}{1 - 1/\tanh x + 1/x} \quad (4)$$

with $x = JS(S+1)/T$, diverges as T^{-2} in the limit $T \rightarrow 0$, while the one for the $S = 1/2$ model, asymptotically given by [17]

$$\chi_s(T) \simeq \frac{c_1}{T} \sqrt{\ln\left(\frac{\Lambda J}{T}\right) + \frac{1}{2} \ln \ln\left(\frac{\Lambda J}{T}\right)}, \quad (5)$$

exhibits only a $1/T$ divergence with logarithmic corrections. Here we note that the quantitative accuracy of this

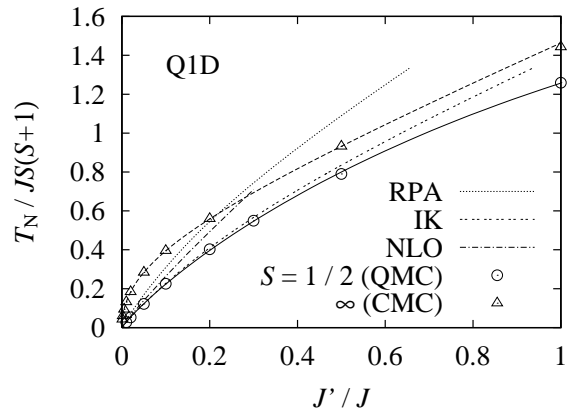


FIG. 1: J' -dependence of $T_N/JS(S+1)$ for the Q1D systems. The open symbols denote our MC results. The error bar of each point is much smaller than the symbol size. The dashed curve passing through the $S = \infty$ data is obtained by Eq. (2) with $k_1=0.7$ and Eq. (4) for χ_s . The solid curve denotes the proposed empirical formula of Eq. (8). The other curves are results of various approximations discussed in the text.

expression is limited to a very low temperature range. In fact Eq. (5) with the constants c_1 and Λ derived field-theoretically [17] does not fit well to χ_s calculated numerically at $T \geq 0.003J$. This indicates the limits of applicability of analytical results and that one has to use instead numerical data in this temperature range.

Due to the different functional forms of the quantum and classical susceptibilities, we observe in Fig. 1 that, at small J'/J , $T_N(J') \propto \sqrt{J'/J}$ for the classical model, while $T_N(J') \propto J'/J$ with logarithmic corrections for the quantum model. Comparing the RPA result (Eq. (2) with $k_1 = 1$) with the modified RPA one (Eq. (2) with $k_1 \simeq 0.70$, denoted by IK), one can easily see that the latter describes $T_N(J')$ much better and is a fairly good description of $T_N(J')$ in the range $J'/J \lesssim 0.3$. Comparing our results to the next leading order finite-temperature perturbation theory [4] (NLO in Fig. 1) which is based on Eq. (5), however, we do not find good agreement, because, as pointed out above, Eq. (5) is inappropriate in the considered temperature range.

The agreement with the modified RPA theory is directly shown in Fig. 2 where the J' -dependence of $\zeta(J')$ in Eq. (1) is shown. The $\chi_s(T_N(J'))$ are obtained from QMC simulations interpolated near $T = T_N$ for the $S = 1/2$ model and from Eq. (4) for the $S = \infty$ model. For $J'/J \leq 0.1$ we reach Eq. (2) with $k_1 \simeq 0.695$ for the $S = 1/2$ model as well as for the classical limit $S = \infty$ model and conclude that, within the numerical accuracy of our simulation, the modified RPA with J' -independent $\zeta(J')$ is an appropriate quantitative description of the models with J'/J in this range.

Interestingly the result mentioned above seems to hold for quantum models with other values of S . As also shown in Fig. 2, within our numerical accuracy, this is

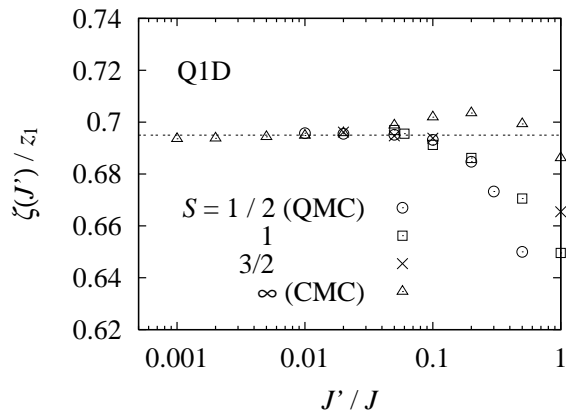


FIG. 2: J' -dependence of $\zeta(J')/z_1$ for the Q1D systems. In all cases $\zeta(J')/z_1$ approaches a constant ($\simeq 0.695$), denoted by the dotted line, at small J'/J . The error bar of each point is smaller than the symbol size.

well confirmed for the $S = 3/2$ model with $J'/J \geq 0.02$. For the $S = 1$ case we find agreement in the range $J'/J \geq 0.05$, where T_N is larger than the Haldane gap [18] of the isolated chain. Below this temperature the finite size scaling of the QMC data becomes less reliable and we cannot draw definitive conclusions. Even if the result for the $S = 1$ model is restricted to this temperature range, the present result is surprising, given the different behavior of $\chi_s(T)$ in the c-1D and q-1D models.

Q2D systems.— In both classical 2D (c-2D) and quantum 2D (q-2D) models, AF-LRO appears at $T = 0$, together with an exponential divergence of $\chi_s(T)$ at $T \rightarrow 0$. In the c-2D system, χ_s is proportional to $T^3 \exp(4\pi J/T)$ at low temperatures [19] and our numerical results agree with previous simulations [20]. For the q-2D models, there is a similar exponential divergence at $T \rightarrow 0$. In the renormalized classical regime of the non-linear σ model [21], for example, $\chi_s(T)$ is written as

$$\chi_s(T)J = c_2 T/J \exp(4\pi\rho_s/T), \quad (6)$$

where ρ_s is the spin stiffness and c_2 a constant.

The J' -dependence of T_N for the Q2D models is shown in Fig. 3. We see that $T_N(J') \propto -1/\ln(J'/J)$ at small J'/J in the $S = 1/2$, $S = 1$ and $S = \infty$ models due to the similar exponential forms of χ_s at $T \rightarrow 0$ of the classical and quantum models. Figure 4 shows that again for $J'/J \lesssim 0.05$ the values of $\zeta(J')$ are universal for the quantum and the classical models: $k_2 = 0.65$ in Eq. (2) independent of the spin size S . This confirms the validity of our modified RPA scenario represented by Eqs. (1) and (2) also for the Q2D systems.

If we insert Eq. (6) into Eq. (1) with $\zeta(J') = \zeta_2$, we obtain the following expression of T_N for $J'/J \ll 1$,

$$T_N = 4\pi\rho_s/(b - \ln(J'/J) - \ln(T_N/J)), \quad (7)$$

with $b = -\ln(\zeta_2 c_2)$. This result is compatible with that of the $1/N$ -expansion theory of $T_N(J')$ due to Irkhin *et*

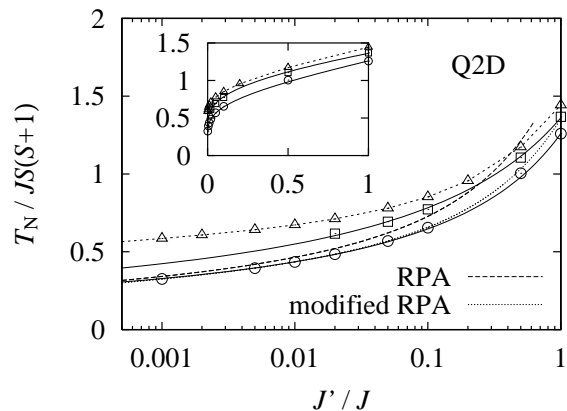


FIG. 3: J' -dependence of $T_N/JS(S+1)$ for the Q2D systems. The open symbols denote our numerical results for the $S = 1/2$ (circles), $S = 1$ (squares), and $S = \infty$ (triangles) models. The error bar of each point is much smaller than the symbol size. The dashed (RPA) and dotted (modified RPA) curves for $S = 1/2$ are obtained from Eqs. (1) and (2) with $k_2 = 1$ and $k_2 = 0.65$, respectively. The solid curves denote the proposed empirical formula (9), while the curve passing through the $S = \infty$ data is simply a guide for the eye. The inset shows the same data on a linear scale.

al. [5] for the $S = 1/2$ model in the same limit. Various estimations of b and ρ_s can be obtained analytically [5] according to the different approximation schemes used. Unfortunately, we cannot judge which approximation is most relevant in general since higher order corrections in $T/4\pi\rho_s$ over the leading asymptotic expression Eq. (7) are known to be necessary [22] to reproduce the numerically obtained χ_s in the temperature range $T/4\pi\rho_s \gtrsim 0.1$ simulated. In fact, corrections of this type and uncertainty on T_N due to the different possible estimates of b are comparable. We expect, on the other hand, that the constancy of the normalization factor k_2 , which is found numerically to be within 2% in $0.001 \lesssim J'/J \lesssim 0.05$ and $0.32 \lesssim T_N/JS(S+1) \lesssim 0.57$ (Fig. 4), holds in the limit $J'/J \rightarrow 0$ as well.

Empirical formulae.— Finally, we propose empirical formulae for $T_N(J')$ based on our QMC results. For the $S = 1/2$ q-Q1D system we propose a modified RPA form based on Eqs. (2) and (5) with a constant $\zeta(J')$,

$$J' = T_N/(4c\sqrt{\ln(\frac{\lambda J}{T_N}) + \frac{1}{2}\ln\ln(\frac{\lambda J}{T_N})}), \quad (8)$$

but with modified values of the constants with $c = 0.233$ and $\lambda = 2.6$. These values are chosen to reproduce not $\chi_s(T)$ but $T_N(J')$ in a wide range of J' . This formula describes $T_N(J')$ very well in the whole range of J'/J as shown in Fig. 1, and it can be used to analyze experimental results, e.g. to obtain $J'/J \simeq 0.0007$ for Sr_2CuO_3 from $T_N/J \simeq 0.002$ [6].

For the q-Q2D systems, we find that instead of Eq. (7), the following simpler expression describes T_N better in

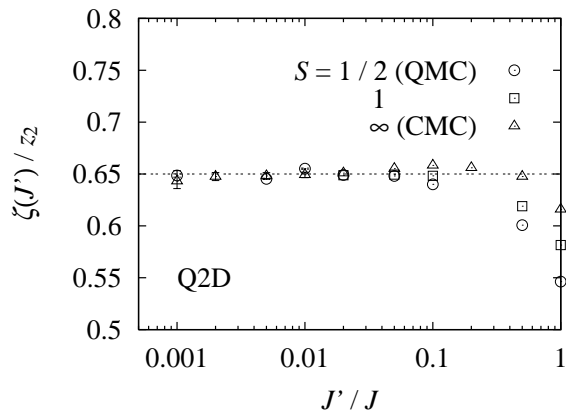


FIG. 4: J' -dependence of $\zeta(J')/z_2$ for the Q2D systems. In all cases $\zeta(J')/z_2$ approaches a constant ($\simeq 0.65$), denoted by the dotted line, at small J'/J . The error bar of each point is smaller than the symbol size unless given explicitly.

TABLE II: Inter-layer coupling J' estimated by Eq. (9) for various infinite-layer compounds. The Néel temperatures T_N , the intra-layer couplings J , and their ratio estimated by the experiments are also listed.

Compound	T_N	J	T_N/J	J'/J
$\text{Ca}_{0.85}\text{Sr}_{0.15}\text{CuO}_2$ [9]	537K	1535K	0.35	0.016
$(5\text{CAP})_2\text{CuBr}_4$ [10]	5.08K	8.5K	0.60	0.24
$(5\text{MAP})_2\text{CuBr}_4$ [10]	3.8K	6.5K	0.58	0.22
$(5\text{CAP})_2\text{CuCl}_4$ [10]	0.74K	1.14K	0.64	0.33
$(5\text{MAP})_2\text{CuCl}_4$ [10]	0.44K	0.76K	0.57	0.21

the range $0.001 \leq J'/J \leq 1$ (see Fig. 3):

$$T_N = 4\pi\rho_s / (b - \ln(J'/J)), \quad (9)$$

with $\rho_s/J = 0.183$ and $b = 2.43$ for $S = 1/2$, and $\rho_s/J = 0.68$ and $b = 3.12$ for $S = 1$. Table II shows inter-layer couplings J' estimated using this equation for a number of infinite-layer materials with $S = 1/2$.

To conclude, we have determined, by high-precision Monte Carlo simulations, the Néel temperatures of quantum and classical Q1D and Q2D Heisenberg antiferromagnets. Besides finding empirical formulae for $T_N(J')$, we observe that, using numerically accurate values of the staggered susceptibility a modified RPA with the J' -independent renormalized coordination number ζ_d succeeds in quantitatively describing the relation between T_N and J'/J for $J' < J'_c$ with $J'_c \simeq 0.1J$.

An intriguing result of our simulations is the independence of ζ_d on the value of the spin S , suggesting a universality of corrections to RPA for $J' \ll J$. Since in this temperature regime the physics of all these models should be well described by an anisotropic non-linear σ -model (NL σ M) in the renormalized classical regime, we conjecture universal corrections to RPA also for the NL σ M.

We acknowledge fruitful discussions with C.P. Landee and M. Matsumoto, and thank M. Bocquet for useful

discussions and for sending his NLO results. Most of the numerical calculations have been performed on the SGI 2800 at Institute for Solid State Physics, University of Tokyo. The program is based on ‘Looper version 2’ developed by S.T. and K. Kato and ‘PARAPACK version 2’ by S.T. This work is supported by Grant-in-Aid for Scientific Research Programs (#12640369, #15740232) and 21st COE Program from the Ministry of Education, Science, Sports, Culture and Technology of Japan, and by the Swiss National Science foundation.

- [1] N. D. Mermin and H. Wagner, Phys. Rev. Lett. **17**, 1133 (1966).
- [2] D. J. Scalapino, Y. Imry, and P. Pincus, Phys. Rev. B **11**, 2042 (1975); H. J. Schulz, Phys. Rev. Lett. **77**, 2790 (1996).
- [3] V. Yu. Irkhin and A. A. Katanin, Phys. Rev. B **61**, 6757 (2000).
- [4] M. Bocquet, Phys. Rev. B **65**, 184415 (2002).
- [5] V. Yu. Irkhin and A. A. Katanin, Phys. Rev. B **55**, 12318 (1997); *ibid.* **57**, 379 (1998); V. Yu. Irkhin, A. A. Katanin, and M. I. Katsnelson, *ibid.* **60**, 1082 (1999).
- [6] A. Keren *et al.*, Phys. Rev. B **48**, 12926 (1993); T. Ami *et al.*, *ibid.* **51**, 5994 (1995).
- [7] B. Keimer *et al.*, Phys. Rev. B **45**, 7430 (1992).
- [8] P. Sengupta, A. W. Sandvik, and R. R. P. Singh, Phys. Rev. B **68**, 094423 (2003).
- [9] T. Siegrist *et al.*, Nature (London), **334**, 231 (1988); D. Vakhnin *et al.*, Phys. Rev. B **39**, 9122 (1989); Y. Tokura *et al.*, *ibid.* **41**, R11657 (1990).
- [10] F. M. Woodward *et al.*, Phys. Rev. B **65**, 144412 (2002).
- [11] H. G. Evertz, G. Lana, and M. Marcu, Phys. Rev. Lett. **70**, 875 (1993); B. B. Beard and U.-J. Wiese, *ibid.* **77**, 5130 (1996); K. Harada, M. Troyer and N. Kawashima, J. Phys. Soc. Jpn. **67**, 1130 (1998); S. Todo and K. Kato, Phys. Rev. Lett. **87**, 047203 (2001).
- [12] U. Wolff, Phys. Rev. Lett. **62**, 361 (1989); Nucl. Phys. B **322**, 759 (1989).
- [13] F. Cooper, B. Freedman, and D. Preston, Nucl. Phys. B **210** [FS6], 210 (1982).
- [14] K. Chen, A. M. Ferrenberg, and D. P. Landau, Phys. Rev. B **48**, 3249 (1993).
- [15] L. Hulthén, Arkiv. Mat. Astron. Fysik **26A**, No. 11 (1938); J. des Cloizeaux and J. J. Pearson, Phys. Rev. **128**, 2131 (1962).
- [16] T. Nakamura, J. Phys. Soc. Jpn. **7**, 264 (1952); M. E. Fisher, Amer. J. Phys. **32**, 343 (1964).
- [17] V. Barzykin, Phys. Rev. B **63**, 140412(R) (2001).
- [18] F. D. M. Haldane, Phys. Lett. **93A**, 464 (1983); Phys. Rev. Lett. **50**, 1153 (1983).
- [19] E. Brézin and J. Zinn-Justin, Phys. Rev. B **14**, 3110 (1976).
- [20] J. Apostolakis, C. F. Baillie, and G. C. Fox, Phys. Rev. D **43**, 2687 (1991).
- [21] S. Chakravarty, B. I. Halperin, and D. R. Nelson, Phys. Rev. B **39**, 2344 (1989); P. Hasenfratz and F. Niedermayer, Z. Phys. B **92**, 91 (1993).
- [22] J-K. Kim and M. Troyer, Phys. Rev. Lett. **80**, 2705 (1998); B. B. Beard *et al.*, *ibid.* **80**, 1742 (1998).